Vibration-based damage detection of structure's joints in presence of uncertainty

Hussein Al-Bugharbee[1,*], *Ali Abolfathi*[2], and *Irina Trendafilova*[3]

[1]Dept. of Mechanical Engineering, University of Wasit, Iraq.
[2] Dept. of Mechanical Engineering, University College London, London, UK.
[3]Mechanical and Aerospace Engineering, University of Strathclyde, Glasgow, UK

Abstract. Early damage detection of structure's joints is essential in order to ensure the integrity of structures. Vibration-based methods are the most popular way of diagnosing damage in machinery joints. Any technique that is used for such a purpose requiers dealing with the variability inherent to the system due to manufacturing tolérances, environnemental conditions or aging. The level of variability in vibrational response can be very high for mass-produced complex structures that possess a large number of components.In this study, a simple and efficient time frequency method is proposed for detection of damage in connecting joints. The method suggests using singular spectrum analysis for building a reference space from the signals measured on a healthy structure and then compares all other signals to that reference space in order to detect the presence of faults. A model of two plates connected by a series of mounts is used to examine the effectiveness of the method where the uncertainty in the mount properties is taken into account to model the variability in the built-up structure. The motivation behind the simplified model is to identify the faulty mounts in trim-structure joints of an automotive vehicle where a large number of simple plastic clips are used to connect the trims to the vehicle structure.

1 Introduction

Joints such as clips and bolts are commonly used in the built-up structures to connect different components. The damage in these joints can adversely affect the integrity of the whole structure and may lead to catastrophic incidents. Thus, an early detection of damage in the structure with faulty joints is a very important task to maintain the safety and to extend the service life span of structures.

Damage detection in structural joints has attracted quite some attention and many techniques were developed during the past few decades. Vibration-based analysis is the most popular strategy for the damage detection because it is non-destructive and repeatable one. The deviation of natural frequency and damping ratios from a baseline values due to bolt looseness is investigated in [1] where a couple of Euler beams with a single bolted lap joint is used in the analysis. The results illustrate that the bolts looseness affect the structure's natural frequencies and damping ratios. However, the change is more significant at the higher frequency range.

In reference [2], an experimental investigation is conducted for identifying the looseness in cargo bolts under random excitation. The experiment is conducted on twelve bolts group and seven different severity of damages (i.e. looseness) are simulated in the experiment. For each simulated damage type, vibration signals are acquired using accelerometer and time series are used for detection. Two kinds of autoregressive models were constructed. The residual errors of the models are used as damage index for different levels of damage. The results showed that the suggested methodology has the possibility of early detection of bolt looseness severity.

A damage detection method based on the analysis of the subharmonic resonance is presented in [3]. The study proposed the structure bolted joint as a two-degree of freedom nonlinear model and uses a multiple timescale method for illustrating the generation of subharmonic resonance. Experiments were conducted on a single bolt-joint aluminum beam and the damage in the joint is simulated by bolts looseness. The excitation of the beams and acquisition of the corresponding response signals are conducted by piezoelectric transducers. The results showed that the subharmonic frequencies appear in the structure response spectrum when it is excited by a double of its natural frequency.

The study in [4] presents a technique for the looseness detection of bolted structure. The technique based on the frequency response function (FRF) data. The experimental results of the study are obtained from two sensors; accelerometer and strain gauge are compared to assess the bolt looseness. The results show that presence of bolt looseness causes and abrupt change in the orthogonal modes.

The detection of undesired structural changes in space

* Corresponding author: hrazzaq@uowasit.edu.iq, husseinmec@yahoo.com

vehicle due to bolt looseness is also investigated in [5]. Special kind of piezoelectric sensors are used on a real satellite panel with 49 bolts. The damage in the satellite panel is simulated as looseness in a bolt. The capability of two different methods, namely Acousto-Elastic and Electro-Mechanical Impedance methods, of detecting damage is investigated. The experimental results of the study show that the present techniques have a potential possibility for both damage detection and localization.

A combined methodology based on vibration and electro-mechanical impedance techniques for the purpose of structural joint damage detection is presented in [6]. A number of structure joint damage scenarios are designed in the study for the purpose of damage detection. The experimental results such as modal parameters are analyzed and showed that the present methodology is useful in extracting a damage information on the structure joint.

The study in Ref. [7] proposes a artificial neural network ANN-based method for the estimation of damage severities in truss bridge's joint. The mode shapes and natural frequencies are used as input features to the ANN in order to assess the damage. For the demonstration of the method efficiency and accuracy, a numerical analysis is presented.

The motivation of the current study is to detect damages in small plastic clips that are used to connect the trim to the structure of an automotive vehicle. A large number of these clips are used in modern vehicles. These clips should be firmly connected and any rattling can be a source of unwanted noise in a vehicle's cabin. It is shown that the variability in the effective stiffness and damping of such clips can affect the vibration response of the vehicle [8]. Such variability makes the damage detection process more difficult and uncertain. In this study, a simple analytical model of two connected plate is used to investigate the possibility of detection of joints in built-up structure in presence of inherent variability in the joints properties. A simple and easy methodology based on Singular Spectrum Analysis (SSA) is suggested here for this purpose. In this method, the time domain vibration acceleration signals are subjected to the SSA for the decomposition purposes. From the response of structure with healthy joints a reference space is made. Other signals of the healthy structure will be projected onto this space and allow an estimation of threshold value. Any new signal will be projected on that baseline space and their distance to the cluster of healthy signal will be compared to the threshold value to classify them as healthy or damaged.

In the following section, the mathematical formulation of the problem is described. In section 3, the fundamentals of the SSA are described briefly. Results and discussion are presented in section 4 and the section 5 focuses on conclusions made in this paper.

2 Mathematical formulation of the problem

A simple model of two connected steel plates with multiple mounts is used here in order to simulate a built-up structure with multiple joints. For the purposes of modeling, the steel plates are simply supported and thus an analytical solution for their vibration response exists according to Kirchhoff–Love plate theory [9]. The two plates are connected by eleven mounts which are distributed randomly between the plates. This allows obtaining an analytical solution using the impedance-mobility technique (FRF coupling) [10][11] The plates are made of steel and have the following dimensions: plate 1 has a thickness of 1.5 mm, width of 350mm and length of 500mm; plate 2 has a thickness of 1.3mm, width of 400mm and length of 600mm. A schematic view of two plates is shown in figure 1.The mobility functions between point 1 on the first plate and point 2 on the second plate are obtained.

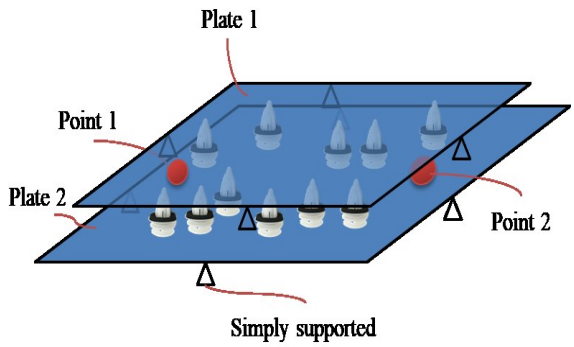

Fig. 1. A schematic view of two plates connected by eleven clips.

The uncertainty in the clips properties are considered based on the measurement conducted in [8]. A Monte Carlo simulation is used to obtain the point and the transfer mobilities while the clips properties are varied. The mobility Y_{12} for point 1 of the first plate and point 2 of the second plate is shown in figure 2 for 250 realisations where all clips are considered connected. It can be seen that at lower frequencies there are distinct modes which are not affected by the variability in clips properties . However, the effect of variability in the clips properties becomes more prevalent at with the increase of the frequencies.

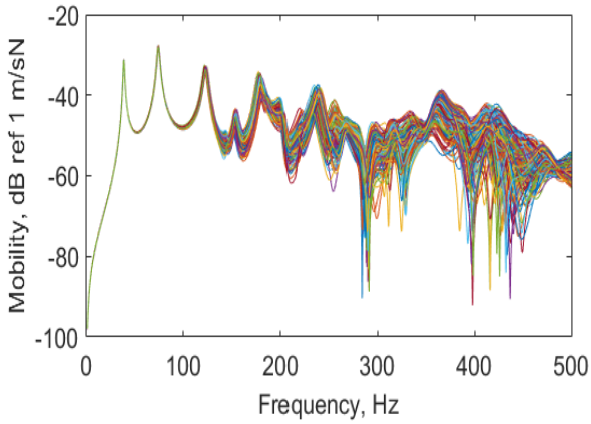

Fig. 2. Monte Carlo simulation results of mobility Y_{12} of two connected plate with 11 clips.

Damage is modelled by removing one clip at a time. Then again a Monte Carlo simulation is used to simulate the

effect of uncertainty in the clip properties. The mobility Y_{12} for the two connected plates, where one of the clips is removed is shown in figure 3. Here, again 250 realizations for each case are produced. Overall 11 cases of damage and one case with no damage are presented in figure 3. . The variability in the clips properties make it impossible to distinguish between each case and there are overlap between healthy and damaged connector for all the cases.

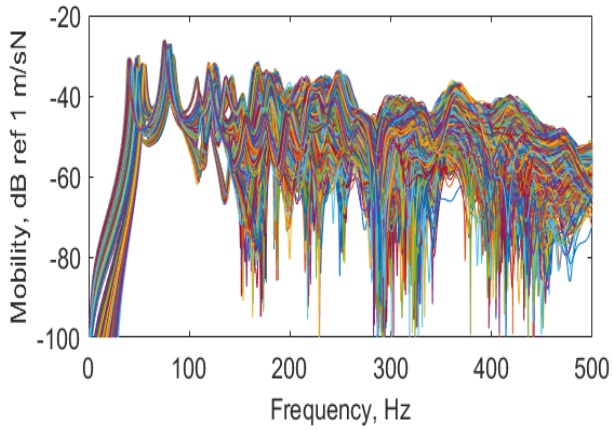

Fig. 3. Monte Carlo simulation of the mobility Y_{12} of two connected plate for healthy and damaged connections where one of the clips is removed each time.

3 Methodology

SSA is a time series analysis method that popularly used in biomedical and meterological sciences [12-14]. Recently, it was used for the purposes of engineering application such as fault diagnosis of rolling element bearings [15-19], tool wear health monitoring [20, 21] and delamination in composite materials [22].

The SSA has two main stages; decomposition and reconstruction. In the first stage, a signal which is discretized as a time series is decomposed into a number of independent components, the principal components (PC's). Each component contains a certain percentage of the original signal variance. The reconstruction stage, which is not used in this methodology, uses all or some of the principal components to reconstruct the original signal. Further details of the SSA can be found in [23, 24].

The methodology suggested has two key steps: building baseline space and damage detection methodology. The later contains extraction of feature vectors (FVs), setting a threshold and a classification process.

3.1 Building reference/baseline space.

A baseline space is made from subjecting a signal measured on a healthy structure to the decomposition stage of the SSA. First a trajectory matrix **X** of dimension (LXK) is made from the time-lapped signal x of a length n (i.e $x = [x(1), x(2), x(3) \dots x(n)]$) as shown in Eq. (1):

$$\mathbf{X} = \begin{bmatrix} x(1) & x(2) & x(3) & \dots & x(K) \\ x(2) & x(3) & x(4) & \dots & x(K+1) \\ x(3) & x(4) & x(5) & \dots & x(K+2) \\ \vdots & \vdots & \vdots & \ddots & \vdots \\ x(L) & x(L+1) & x(L+2) & \dots & x(K+L-1) \end{bmatrix} \quad (1)$$

where $x(n)$ is a nth element of the measured signal. The L is the window of decomposition (i.e the number of PCs resulted from the decomposition stage) and $K=n-L+1$. The covariance matrix of the trajectory matrix can be obtained according to Eq. 2.

$$\mathbf{C}_{\mathrm{x}} = \frac{\mathbf{X}\mathbf{X}'}{L} \quad (2)$$

Then it is subjected to singular value decomposition as shown in Eq.3 to obtain its eigenvalues and eigenvectors,

$$\mathbf{C}_x \mathbf{U}_i = \lambda_i \mathbf{U}_i \quad (3)$$

Each eigenvalue (i.e. λ_i) represents a fraction of the original signal's variance in the direction of the corresponding eigenvector $\mathbf{U}_i$. The eigenvalues are usually arranged in a decreasing order and the corresponding variances are represented in the so-called scree plot [25].

For building the baseline space, all or only a part of eigenvectors obtained above, which correspond to the healthy condition can be used.

3.2 Damage detection methodology

After building the baseline/reference space from healthy signals, any new signals will be projected on the baseline space and the fault detection process is conducted. The detection process has two main steps: feature vector extraction and classification.

3.2.1 Feature vector extraction

Supposing signals from healthy and faulty condition are available, the healthy signals are divided equally into a training and a testing sample, while all the faulty signals are used as testing sample.

For the training sample, the trajectory matrix of every signal is projected onto the baseline space. The projection means multiplying the transpose of the trajectory matrix **X** by each of the baseline eigenvector $\mathbf{U}_i$. This projection will provide the corresponding principal components $\mathbf{PC}_i$ as in Eq.4

$$\mathbf{PC}_{i_i} = \frac{\mathbf{X}'\mathbf{U}_i}{\lambda_i} \quad (4)$$

The symbol ($'$) denotes the transpose. Then, the Euclidean norm of each of the three principal components is calculated as in Eq.5,

$$f_{ij} = \sum_{m=1}^{K} \left(\mathbf{PC}_{ij}\,(m)\right)^2 \quad (5)$$

where f_{ij} is the feature, i is the number of principle component and j is the number of the signal that is

projected. .

In the present study, the baseline space is basically made from the first three eigenvectors. Hence, all feature vectors will be of three dimensions. More eigenvectors can also be used but in this study the first three vectors were sufficient to achieve a very good classification . Then the feature vectors obtained from j^{th} signal will have the form,

$$\mathbf{f}_j = [f_{1j}\ \ f_{2j}\ \ f_{3j}]' \qquad (6)$$

The reason for choosing three feature components only is that these can be visualized in a 3D space.

3.2.2 Classification

When a baseline space is made and the training samples are projected, the resultant FVs are arranged in rows to form the baseline feature matrix $\mathbf{F}_{baseline}$,. Then, the Mahalanobis distance $(D_i)$of each feature vector to the $\mathbf{F}_{baseline}$ is calculated as shown in Eq.7.

$$D_i = \sqrt{(fv_i - E_{baseline}).S^{-1}.(fv_i - E_{baseline})^T} \quad (7)$$

Where $\mathbf{E}_{baseline}$ is the mean of the rows of the $\mathbf{F}_{baseline}$.andS^{-1} is the inverse of the covariance matrix of $\mathbf{F}_{baseline}$.

From the values of D_i corresponding to the baseline training sample a suitable probability distribution is fitted. In the present study, a lognormal probability distribution if fitted. From this probability distribution a suitable threshold T_r is found. The threshold here is selected as the value for which the cumulatve probability distribution equals 0.99 [26].. A new signal will be classified based on its D_i to the class of healthy or faulty signals, according to the Eq.8.

$$\begin{aligned} &D_i > T_r \quad \textit{singal is assigned to healthy class} \\ &D_i \leq T_r \quad \textit{signal is assigned to faulty class} \end{aligned} \qquad (8)$$

where D_i is the Mahalanobis distance of ith signal measured from the healthy space and T_r is the calculated threshold.

4 Results and discussion

As was mentioned in Section 3 250 realizations were obtained for the case when all clips are mounted that is for the case of healthy clips. Similarly 250 signlas are recorded for each case when one clip is removed. In total there will be 3000 realizations (250*12 (1 Healthy case +11 removed clip cases)). The signals from the healthy structure are divided equally (i.e each is 125 relaisations) into a training and a testing sample, each on containing 125 signals. All the other 2750 signals are used as a testing sample.

Figure 1 represents the 3D visualization of training FVs which were obtained according to Eq.6.

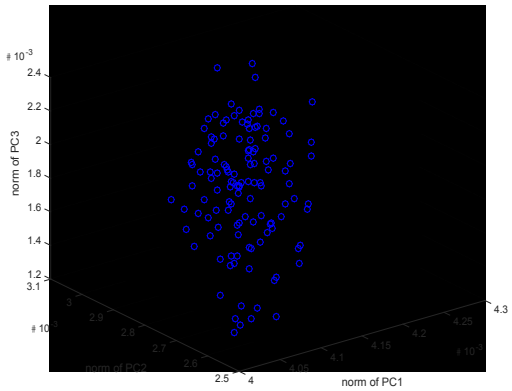

Fig. 1. 3D visualisation of baseline FVs.

Figure 2 shows the projection of the testing FVs on the baseline feature space. The healthy training and testing FVs are represented in blue color. The FVs corresponding to faulty class are represented in red color. It can be seen that the testing FVs corresponding to the faulty cases can be visually recognized from the baseline FVs.

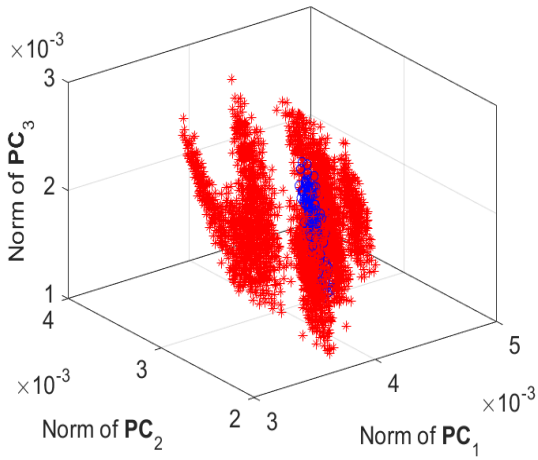

Fig. 2. Clustering of 3D visualisation of baseline FVs.

The Figure 3 represents the *D* values of the Mahalanobis distances of all the feature vectors that were measured to the training FVs. The horizontal dashed line represents the threshold *Tr*. The figure clearly shows that the *D* level of the faulty FVs is higher than the *D* level of the training FVs. In this sense the FVs made from faulty class are dissimilar to those made from training FVs. The FV's from the faulty class will be recognized as such according the rule defined in equation (8)

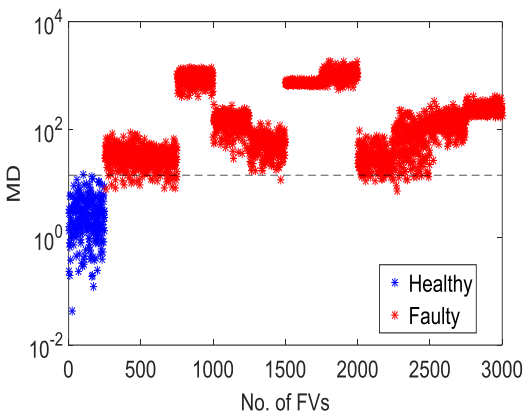

Fig. 3. The levels of *D* for both training and testing sample.

Table 2 shows the confusion matrix that represents the rates of correct and incorrect classification in percents for the healthy and the faulty signals. The first column denotes the real class and the first row corresponds to the recognized class. The numbers on the main diagonal shows the correct classification rates while the off diagonal numbers show the percentage of misclassified signals r. It can be seen that all the 125 healthy FVs from the testing sample are correctly assigned to the healthy class. From the table it can be seen that only 31 out of the 2750 (1.13 %) testing FVs corresponding to faulty conditions were misclassified as healthy while all the rest 2719 FVs (i.e 98.87%) were correctly classified as faulty.

Table 2. Confusion matrix

Real class/recognized class	**H**	**F**
H	100%	0%
F	1.13%	98.87%

5 Conclusions

This study suggests a vibration-based monitoring method for small plastic clips used to connect the trim to the structure of an automotive vehicle. It was shown that damage in one of this clips or a missing clip affects the vibration signal measured on the vehicle. Currently such clips are not monitored but any damage in the clips or any unscrewed or missing clip will cause unwanted noise in the vehicle. This is why this study suggests to monitor the condition of such clips and fix them on the basis if the results of this monitoring. In this study a simple but efficient methodology for damage detection in these small plastic clips in automotive vehicle is developed

The methodology does not require previous measurements of signals corresponding to faulty cases and it is able to distinguish not only between healthy and faulty signals but also among different faulty cases. The results obtained in the paper demonstrate the accuracy of the method, which supports the claim of using it for purposes of automatic of damage assessment.

References

1 A. D. A. R. A. G. G. K. V, "Bolted Lap Joint Structure: Structural Health Monitoring Using Damping Ratio as Indicator," presented at the 2nd Mechanical Engineering Graduate Research Symposium (MEGRES), IIT Bombay, Mumbai, India, 2015.

2 G. Dong, F. Zhao, and X. Zhang, "Experimental study on monitoring the bolt group looseness in a clamping support structure model," *Advances in Mechanical Engineering,* vol. **9**, p. 1687814017695046, (2017).

3 M. Zhang, Y. Shen, L. Xiao, and W. Qu, "Application of subharmonic resonance for the detection of bolted joint looseness," *Nonlinear Dynamics,* vol. **88**, pp. 1643-1653, (2017).

4 H.-C. Eun, Y.-J. Ahn, and S.-G. Lee, "Experimental study on damage detection at bolted joint using frequency response function."

5 D. Doyle, A. Zagrai, and B. Arritt, "Bolted joint integrity for structural health monitoring of responsive space satellites," in *Proceedings of the Proceeding of 50th AIAA/ASME/ASCE/AHS/ASC Structures, Structural Dynamics, and Materials Conference, Palm Springs, CA*, 2009.

6 W. Na, J. Lee, J. Kim, and D. Hong, "Hybrid Health Monitoring for Damage Detection in Structural Joints," (2006).

7 M. Mehrjoo, N. Khaji, H. Moharrami, and A. Bahreininejad, "Damage detection of truss bridge joints using Artificial Neural Networks," *Expert Systems with Applications,* vol. **35**, pp. 1122-1131, (2008).

8 A. Abolfathi, D. J. O'Boy, S. J. Walsh, A. M. Dowsett, and S. A. Fisher, "The uncertainty in stiffness and damping of an automotive vehicle's trim-structure mounts and its effect on the variability of the vibration transfer function," *Proceedings of the Institution of Mechanical Engineers, Part C: Journal of Mechanical Engineering Science,* p. 0954406217721724, (2017).

9 S. S. Rao, *Vibration of continuous systems*: John Wiley & Sons, 2007.

10 P. Gardonio and M. Brennan, *Mobility and impedance methods in structural dynamics* vol. 9: chapter, 2004.

11 E. L. Hixson, "Mechanical impedance," *Shock and vibration handbook,* vol. **10**, pp. 1-46, (1988).

12 S. Sanei and H. Hassani, *Singular spectrum analysis of biomedical signals*: CRC Press, 2015.

13 S. M. Mohammadi, S. Enshaeifar, M. Ghavami, and S. Sanei, "Classification of awake, REM, and NREM from EEG via singular spectrum

analysis," in *2015 37th Annual International Conference of the IEEE Engineering in Medicine and Biology Society (EMBC)*, 2015, pp. 4769-4772.

14 A. Hossein Vahabie, M. M. R. Yousefi, B. N. Araabi, C. Lucas, and S. Barghinia, "Combination of singular spectrum analysis and autoregressive model for short term load forecasting," in *Power Tech, 2007 IEEE Lausanne*, 2007, pp. 1090-1093.

15 B. Kilundu, X. Chiementin, and P. Dehombreux, "Singular spectrum analysis for bearing defect detection," *Journal of Vibration and Acoustics,* vol. **133**, p. 051007, (2011).

16 T. Liu, J. Chen, and G. Dong, "Singular spectrum analysis and continuous hidden Markov model for rolling element bearing fault diagnosis," *Journal of Vibration and Control,* pp. 1506-1521, (2013).

17 B. Muruganatham, M. Sanjith, B. Krishnakumar, and S. Satya Murty, "Roller element bearing fault diagnosis using singular spectrum analysis," *Mechanical Systems and Signal Processing,* vol. **35**, pp. 150-166, (2013).

18 H. Al-Bugharbee and I. Trendafilova, "A fault diagnosis methodology for rolling element bearings based on advanced signal pretreatment and autoregressive modelling," *Journal of Sound and Vibration,* vol. **369**, pp. 246-265, (2016).

19 H. Al-Bugharbee and I. Trendafilova, "A new methodology for fault detection in rolling element bearings using singular spectrum analysis," *International Journal of Condition Monitoring,* vol. **7**, pp. 26-35, (2017).

20 D. Salgado and F. Alonso, "Tool wear detection in turning operations using singular spectrum analysis," *Journal of Materials Processing Technology,* vol. **171**, pp. 451-458, (2006).

21 B. Kilundu, P. Dehombreux, and X. Chiementin, "Tool wear monitoring by machine learning techniques and singular spectrum analysis," *Mechanical Systems and Signal Processing,* vol. **25**, pp. 400-415, (2011).

22 D. Garcia, I. Trendafilova, and H. Al-Bugharbee, "Vibration-based health monitoring approach for composite structures using multivariate statistical analysis," in *EWSHM-7th European workshop on structural health monitoring*, 2014.

23 N. Golyandina and A. Zhigljavsky, *Singular Spectrum Analysis for time series*: Springer Science & Business Media, 2013.

24 H. Hassani, "Singular spectrum analysis: methodology and comparison," (2007).

25 L. Zhang, J. Marron, H. Shen, and Z. Zhu, "Singular value decomposition and its visualization," *Journal of Computational and Graphical Statistics,* vol. **16**, pp. 833-854, (2007).

26 H. R. Al-Bugharbee, "Data-driven methodologies for bearing vibration analysis and vibration based fault diagnosis," University of Strathclyde, 2016.